Gigahertz longitudinal acoustic phonons originating from ultrafast ligand field transitions in hematite thin films*

Xu Yue(徐 悦)[a], Jin Zuan-Ming(金钻明)[a)b)], Zhang Zheng-Bing(张郑兵)[a)], Zhang Ze-Yu(张泽宇)[a)], Lin Xian(林 贤)[a)], Ma Guo-Hong(马国宏)[a)†], and Cheng Zhen-Xiang(程振祥)[c)‡]

[a)] *Laboratory of Ultrafast Photonics, Department of Physics, Shanghai University, Shanghai* 200444, *China*
[b)] *Max Planck Institute for Polymer Research, Ackermannweg* 10, 55128 *Mainz, Germany*
[c)] *Institute for Superconductor and Electronic Materials, University of Wollongong, Squires Way, North Wollongong, NSW* 2500, *Australia*

(Received 12 June 2013; revised manuscript received 11 August 2013; published online 10 February 2014)

The creation and propagation of longitudinal acoustic phonons (LAPs) in high quality hematite thin films (α-Fe_2O_3) epitaxially grown on different substrates ($BaTiO_3$, $SrTiO_3$, and $LaAlO_3$) are investigated using the femtosecond pump–probe technique. Transient reflection measurements ($\Delta R/R$) indicate the photo-excited electron dynamics, and the initial decay less than 1 ps and the slow decay of ~500 ps are attributed to the electron-LO phonon coupling and electron–hole nonradiative recombination, respectively. LAPs in α-Fe_2O_3 film can be created by ultrafast excitation of the ligand field state, such as the ligand field transitions under 800-nm excitation as well as the ligand to metal charge-transfer with 400-nm excitation. The strain modulations of the sound velocity and the out-of-plane elastic properties are demonstrated in α-Fe_2O_3 film on different substrates.

Keywords: α-Fe_2O_3, pump–probe technique, acoustic phonons, ligand field

PACS: 42.50.Md, 78.20.hb, 78.47.J– **DOI:** 10.1088/1674-1056/23/4/044206

1. Introduction

The transduction of light-to-sound with longitudinal acoustic phonons is an active subject of research, providing a new understanding and controlling of fundamental physical properties.[1–3] Much attention has been focused on transition metal–oxide materials in the past five years, because of their interesting electronic, optical, and magnetic properties.[4,5] The electronic and magnetic properties of transition metal oxides are dominated by the electronic and spin states of d-electrons of the transition metal ions under the modulation of the ligand field, provided by oxygen ions, via pressure and temperature.[6,7] It has been proved that the ligand field states can be photo-excited with ultrafast pulses directly. Accordingly, the carrier relaxation, phase transition, and spin dynamics can be modified in transition metal oxides.[8–10] Recently, some groups independently reported in succession that the above-band-gap optical excitation can produce transient acoustic phonons in multiferroic $BiFeO_3$ (BFO) single crystal and thin films, which were measured by ultrafast spectroscopy.[11] Time-resolved X-ray diffraction demonstrated that the structural and electronic responses are strongly related in BFO thin film[12] and $PbZr_{0.2}Ti_{0.8}O_3$ nanolayers.[13]

The α-Fe_2O_3 has attracted a great deal of attention not only for its relatively small band gap (about 2.2 eV), good chemical stability, low toxicity, and easy preparation, but also for its various applications, such as heterogeneous catalyst, pigment, gas sensor, and magnetic material.[14,15] A number of investigations were performed on the ultrafast electronic relaxation dynamics[16,17] and nonlinear optical properties of iron oxide.[18] Although the coherent photo-induced phonons were observed in single crystal[14] and nanocrystal γ-Fe_2O_3 film,[19] there is no report about the generation of acoustic phonons in α-Fe_2O_3 thin film, especially the acoustic phonon propagation characteristics at the interface between the sample and different substrates to the best of our knowledge.

In this study, the standard reflection-type pump–probe setup is employed to create and detect the gigahertz (GHz) longitudinal acoustic phonons (LAPs) in high quality α-Fe_2O_3 thin films epitaxially grown on different substrates. The observed GHz LAPs in α-Fe_2O_3 film originate from the displacement of the metal–ligand equilibrium geometry by ultrafast excitation of the ligand field transition. The strain modulation of sound velocity and out-of-plane elastic properties are demonstrated in α-Fe_2O_3 film on different substrates. Our results indicate that α-Fe_2O_3 would be a favorable material for the ultrafast opto-acoustic devices.

2. Experimental details

Samples used in the present study were the α-Fe_2O_3 thin films on $BaTiO_3$ (BTO), $SrTiO_3$ (STO), and $LaAlO_3$ (LAO) substrates, which were fabricated using a pulsed laser deposition system. The third harmonic generated by an Nd-doped

*Project supported by the National Natural Science Foundation of China (Grant No. 11174195).
†Corresponding author. E-mail: ghma@staff.shu.edu.cn
‡Corresponding author. E-mail: cheng@uow.edu.au
© 2014 Chinese Physical Society and IOP Publishing Ltd

yttrium aluminum garnet laser with a wavelength of 355 nm and a repetition rate of 10 Hz was used as a laser source. The α-Fe_2O_3 thin films with (012)-orientation were deposited on (100)-BTO, (100)-STO, and (100)-LAO at 650 °C with a dynamic oxygen flow and oxygen pressure of 40 Pa. The thickness values of all α-Fe_2O_3films were about (150±30) nm. The selected sample α-Fe_2O_3 on LAO was characterized by absorption spectra and X-ray diffraction as shown in Figs. 1(a) and 1(b).

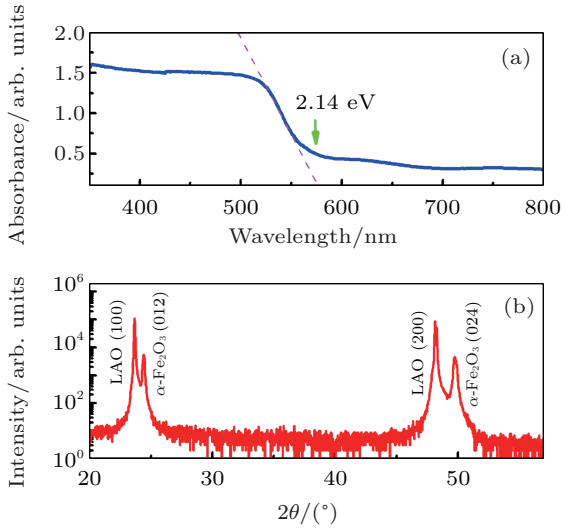


Fig. 1. (color online) Absorption spectrum (a) and X-ray diffraction patterns (b) of the selected sample α-Fe_2O_3 on LAO.

Ultrafast single-, and dual-color pump–probe techniques were performed using laser pulses with a full width at half maximum of 120 fs, delivered from a commercial Ti:sapphire regenerative amplifier (Spectra-Physics Spitfire Pro) with a central wavelength of 800 nm and a repetition rate of 1 kHz. The output pulse train was split into pump and probe beams by a beam splitter. The transmitted intense beam passing through an attenuator acted as a pump beam for the single-color pump–probe study. For the dual-color pump–probe study, the intense pump beam was frequency-doubled in a 1-mm BBO crystal to produce a pumping fluence of ~3.8 mJ/cm^2 at 400 nm (above the band gap of α-Fe_2O_3). The reflected fundamental beam at 800 nm (below the band gap of α-Fe_2O_3) served as a probe beam, whose fluence was less than 0.1 mJ/cm^2. Both the pump beam and the probe beam were focused on the sample surface to a spot with a diameter of about 100 μm for the pump and somewhat smaller for the probe beam. The sample was mounted in a closed-cycle liquid-He cryostat in a vacuum chamber with four optically accessible windows, of which the temperature can be varied in a range from 12 K to 300 K.

3. Results and discussion

Figures 2(a) and 2(b) show the plots of typical transient reflectivity change ($\Delta R/R$) versus delay time of α-Fe_2O_3 thin films on LAO substrate, pumped with two different wavelengths (400 nm and 800 nm) and probed at 800 nm in a short time range (i.e. from –2 ps to 5 ps) and a big time range (i.e. from –2 ps to 100 ps), respectively. Figure 2(c) shows the plots of $\Delta R/R$ versus delay time of α-Fe_2O_3 thin films on three different substrates, pumped with 400 nm and probed with 800 nm in a long time range. Both sets of data exhibit dynamic behaviors occurring on a multiple time scale. Empirically, the main features in the dynamics are due to a sharp initial dropping followed by a fast- (less than 1 ps) and slow-relaxation (about 500 ps), in which the slow relaxation is superimposed on a long-lived damped oscillation process. According to the earlier studies on the ligand field transition, the swift drop of $\Delta R/R$ at zero time delay with pump wavelength at 800 nm may preferentially be triggered by transition from the ground ($^6A_1$) to the excited ($^4T_1$) ligand field state of Fe^{3+} ions.[19] However, the direct and stronger transitions from 2p O^{2-} valence band orbitals to the conduction band edge occur at 3.0 eV–4.7 eV.[16] Therefore, for a pump wavelength of 400 nm, the ligand-to-metal charge-transfer transition is excited, while some excitations involving d–d transitions in Fe^{3+} ion are also possible. The number of excited carriers is expected to be proportional to the pump fluence, which is confirmed by the experimental results that the amplitude of $\Delta R/R$ around zero delay time is linearly dependent on the pump fluence. The very fast-relaxation component, less than

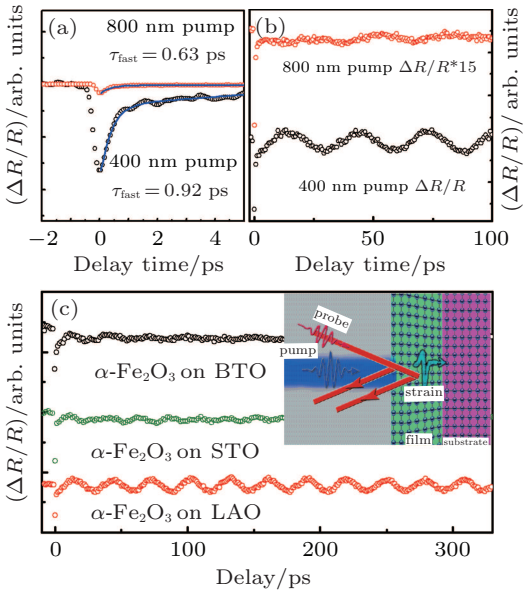


Fig. 2. (color online) (a) Plots of the transient reflectivity change ($\Delta R/R$) versus delay time of α-Fe_2O_3 thin films on LAO substrate, pumped with two different wavelengths (400 nm and 800 nm) and probed with 800 nm in a short time range (i.e. from –2 ps to 5 ps). The dot lines represent the experimental data, and the solid lines represent the fitted curves. (b) The date of $\Delta R/R$ pumped with 800 nm is zoomed in 15 times in a time range from –5 ps to 100 ps. (c) Plots of $\Delta R/R$ versus delay time of α-Fe_2O_3 thin films on three different substrates, pumped with 400 nm and probed with 800 nm. The inset of panel (c) shows the experimental configuration as well as the generation and propagation scheme of coherent acoustic phonons.

1 ps, is possibly corresponding to the hot electrons relaxation: through interacting with longitudinal-optical (LO) phonons, the hot electrons release their energies to reach the bottom of the conduction band.[20] Figure 2(a) shows that the fast relaxation component excited by 800 nm is faster than that pumped with 400 nm, which means that the fast-relaxation component is associated with the high-energy electrons accumulated in different conduction bands by emitting the LO phonons. On the other hand, the slow-relaxation background mainly comes from the contribution of electron–hole nonradiative recombination in α-Fe_2O_3.[16] In the present study, we concentrate on the appearance of the long-lived damped oscillatory features, associated with strain pulse propagation created by the ultrafast optical excitation, which is described below.

As reported on BFO thin films,[11] we deduct the background of the electron relaxation, and then can obtain the pure oscillation component as plotted in Figs. 3(a)–3(c). The frequency of oscillation, named Brillouin frequency remains unchanged with the increasing of the pump fluence, while the amplitude of the oscillation is proportional to the pump fluence. The pure oscillation component can be fitted by a damped harmonic function, $A\cos(2\pi t/T+\phi)\exp(-t/\tau)$, where A, T, τ, and ϕ are the amplitude, period, damping time, and initial phase of the long-lived oscillations, respectively. The dot lines in Figs. 3(a)–3(c) represent the experimental data, and the solid lines denote the fitting results.

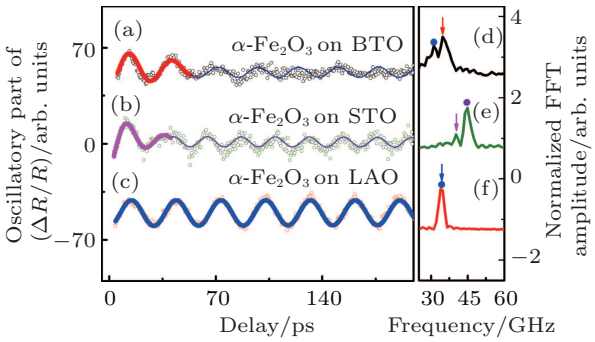


Fig. 3. (color online) Oscillatory parts of $\Delta R/R$ pumped with 400 nm of α-Fe_2O_3 films on substrates of (a) (100)-BTO, (b) (100)-STO, and (c) (100)-LAO. The dot lines represent the experimental data, and the solid lines denote the fitted curves. (d)–(f) The fast Fourier transform (FFT) spectra obtained from $\Delta R/R$ without the relaxation background at room temperature. The arrows point to the Brillouin frequencies of α-Fe_2O_3 on the different substrates. The points represent the Brillouin frequencies of the different substrates.

Coherent phonons are usually excited by either a displacive or impulsive mechanism,[21] depending on the excitation properties of the pump pulse and the electronic structure of the sample. As mentioned above, the LAP can be created by pumping wavelengths of 800 nm and 400 nm. It means that the coherent phonons are associated with the displacement of equilibrium lattice geometry on $^6A_1 \rightarrow {}^4T_1$ and ligand $\rightarrow$ metal charge-transfer excitation, rather than impulsive stimulated Raman scattering. Figure 2(b) shows that the excitation of the coherent phonon via below-band gap ligand field transition (pumped by 800 nm) is less efficient than the charge-transfer transition (pumped by 400 nm), which is consistent with the theoretical prediction. The ligand field transitions have vibronic coupling 5–10 times smaller than the charge-transfer transitions between the metal and ligand.[22,23] Our finding indicates that the ligand field transition pumped with 800 nm is sufficient to excite the LAP in α-Fe_2O_3 film. Further insight into the origin of the displacement of the equilibrium geometry from optical transition, is the change of the electronic configuration in d-orbitals, which can shift an electron from an antibonding to a nonbonding molecular orbital, and consequently reduces the distance of the metal–ligand equilibrium.[24] Looking at Fig. 2(b) closely, the phase of oscillations is somewhat shifted for two different pump wavelengths. This suggests that the time needed to generate strain wave in α-Fe_2O_3 thin film is dependent on the wavelength of the pump pulse. This further raises interesting questions on the efficiency of lattice displacement, owing to different types of optical transitions.

As mentioned above, the strain pulse launches on the surface of the α-Fe_2O_3 thin film due to the displacement of the metal–ligand equilibrium geometry propagating into the bulk, and then causes an oscillation of $\Delta R/R$. The strain pulse is probed by the interference between the probe beams reflected by the thin film surface and the wave front of the propagating strain pulse.[11] The inset of Fig. 2(c) shows the experimental configuration as well as the propagation and detection scheme of the LAP. The propagation of the LAP can be recorded by scanning the time delay between the pump and probe pulses. When the out-of-plane strain pulse propagates across the α-Fe_2O_3/BTO or α-Fe_2O_3/STO interface, a discontinuity in the oscillation feature is clearly observed at the interface. At the same time, it is predicted that the amplitude of oscillation decreases and the Brillouin frequency changes through the interface. By means of the damped harmonic fit, the fast Fourier transform (FFT) of the oscillations are shown in Figs. 3(d)–3(f). The Brillouin frequencies are 35.1 GHz and 30.9 GHz for α-Fe_2O_3 film (thick line) and BTO (thin line), while 40.2 GHz and 44.7 GHz for α-Fe_2O_3 film (thick line) and STO (thin line). The oscillation feature shows nearly uniform amplitude and only one Brillouin frequency of 33.9 GHz is observed between α-Fe_2O_3 film and the LAO substrate, which is possibly because α-Fe_2O_3 thin film and the LAO substrate are perfectly lattice-matched.

According to the strain pulse propagation model,[25] the sound velocity in the sample is given by $v_{\text{sound}} = \lambda_{\text{probe}}/2T\sqrt{n_{\text{probe}}^2 - \sin^2(\theta)}$, where n_{probe}, θ, T, λ_{probe} are the refractive index of α-Fe_2O_3 films at the probe beam wavelength, the incident angle of the probe beam on the sample surface, the period of vibration signal in $\Delta R(t)/R$, and the

wavelength of the probe beam, respectively. In our case, the θ approaches to 0°, and the sound velocity can be reduced to $v_{\text{sound}} = \lambda_{\text{probe}}/2Tn_{\text{probe}}$. On account of the refractive index of α-Fe_2O_3 film ranging from $n = 2.75$ to $n = 2.85$, the sound velocities of the α-Fe_2O_3 thin films on different substrates can be estimated, $v_{\text{sound}} = 4882$ m/s–5060 m/s on (001)-BTO, $v_{\text{sound}} = 5653$ m/s–5858 m/s on (001)-STO, and $v_{\text{sound}} = 4756$ m/s–4929 m/s on (001)-LAO. The longitudinal sound velocity, together with the mass density determines the out-of-plane longitudinal elastic constant, $C_\perp$, by the relation $\rho(v_{\text{sound}})^2 = C_\perp$.[26] The mass density of α-Fe_2O_3 is taken to be $\rho = 5240$ kg·m^{-3}, then $C_\perp = 125$ GPa–134 GPa on (001)-BTO, 167 GPa–180 GPa on (001)-STO, and 118 GPa–127 GPa on (001)-LAO as summarized in Fig. 4(a). Figure 4(b) shows the temperature dependence of the Brillouin frequency of α-Fe_2O_3/LAO, and the Brillouin frequency does not show any change at the temperatures ranging from 300 K to 12 K. The amplitude and the damping time of the oscillation increases significantly with the decrease of temperature, owing to the suppressed thermal phonon–phonon scattering at low temperatures. The iron and oxygen atoms in hematite are arranged in the corundum structure, which is six formula units per unit cell. The arrangement of the oxygen anions and the high-spin cations naturally affect the orientation of the spin magnetic moment of the iron atom. The diverse magnetic properties of all the iron oxides have been recently reviewed.[27] Hematite is antiferromagnetic at temperatures below 260 K and a weak ferromagnetic at room temperature.[28] The temperature-induced magnetic phase transition is not observed from the time-resolved spectrum in the present study.

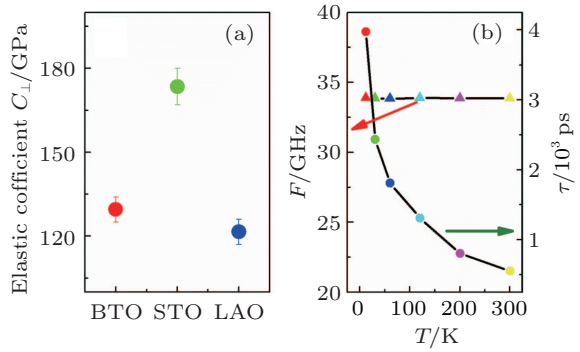


Fig. 4. (color online) (a) Estimated elastic coefficients of α-Fe_2O_3 films on substrates of (100)-BTO, (100)-STO, and (100)-LAO, pumped with 400 nm, respectively, compared with those determined from the Brillouin frequencies and published values of refractive index n from 2.75 to 2.85. (b) Plots of Brillouin frequencies and damping time (τ) of α-Fe_2O_3 films on (100)-LAO versus temperature.

4. Conclusion

In this paper, pump–probe spectroscopy with short-pulsed laser is used to study the generation and propagation of the GHz coherent acoustic phonons in α-Fe_2O_3 thin films on different substrates. The generation mechanism of LAP is strongly related to the ultrafast electron transitions, such as ligand field transitions and ligand-to-metal charge-transfer excitations. Significantly, the strain modulations of sound velocity and out-of-plane elastic properties are demonstrated in α-Fe_2O_3 films on different substrates. As far as applications are concerned, the ultrafast coupling of light with mechanical degrees of freedom guides the promising practical applications in types of photo-driven sensors.

Acknowledgment

Cheng Zhen-Xiang thanks the Australia Research Council for support.

References

[1] Armstrong M R, Reed E J, Kim K Y, Glownia J H, Howard W M, Piner E L and Roberts J C 2009 *Nat. Phys.* **5** 285
[2] Akimov A V, Scherbakov A V, Yakovlev D R, Foxon C T and Bayer M 2006 *Phys. Rev. Lett.* **97** 037401
[3] Hase M, Ishioka K, Demsar J, Ushida K and Kitajima M 2005 *Phys. Rev. B* **71** 184301
[4] Hong F, Cheng Z X, Zhao H Y, Kimura H and Wang X L 2011 *Appl. Phys. Lett.* **99** 092502
[5] Xu Y, Jin Z M, Li G F, Zhang Z B, Lin X, Ma G H and Cheng Z X 2012 *Acta Phys. Sin.* **61** 177802 (in Chinese)
[6] Abal G R, Ney O, Satitkovitchai K and Hubner W 2004 *Phys. Rev. Lett.* **92** 227402
[7] Takano M, Nasu S, Abe T, Yamamoto K, Endo S, Takeda Y and Goodenough J B 1991 *Phys. Rev. Lett.* **67** 3267
[8] Yao G X, Lu L H, Gui M F, Zhang X Y, Zheng X F, Ji X H, Zhang H and Cui Z F 2012 *Chin. Phys. B* **21** 107801
[9] Kimel A V, Kirilyuk A, Usachev P A, Pisarev R V, Balbashov A M and Rasing T 2005 *Nature* **435** 655
[10] Jiang Q, Kang Y T and Yao D X 2013 *Chin. Phys. B* **22** 087402
[11] Jin Z M, Xu Y, Zhang Z B, Lin X, Ma G H, Cheng Z X and Wang X L 2012 *Appl. Phys. Lett.* **101** 242902
[12] Wen H D, Chen P, Cosgriff M P, Walko D A, Lee J H, Adamo C, Schaller R D, Ihlefeld J F, Dufresne E M, Schlom D G, Evans P G, Freeland J W and Li Y L 2013 *Phys. Rev. Lett.* **110** 037601
[13] Korff C V S, Bargheer M, Kiel M, Zhavoronkov N, Woerner M, Elsaesser T, Vrejoiu I, Hesse D and Alexe M 2007 *Phys. Rev. Lett.* **98** 257601
[14] Joly A G, Williams J R, Chambers S A, Xiong G, Hess W P and Laman D M 2006 *J. Appl. Phys.* **99** 053521
[15] Jonathan K L and Allen J B 1987 *J. Phys. Chem.* **91** 5076
[16] Cherepy N J, Liston D B, Lovejoy J A, Deng H M and Zhang J Z 1998 *J. Phys. Chem. B* **102** 770
[17] Pendlebury S R, Barroso M, Cowan A J, Sivula K, Tang J, Gratzel M, Klug D and Durrant J R 2011 *Chem. Commun.* **47** 716
[18] Hashimoto T, Yamada T and Yoko T 1996 *J. Appl. Phys.* **80** 3184
[19] Chen T Y, Hsia C H, Son H S and Son D H 2007 *J. Am. Chem. Soc.* **129** 10829
[20] Krasniqi F S, Johnson S L, Beaud P, Kaiser M, Grolimund D and Ingold G 2008 *Phys. Rev. B* **78** 174302
[21] Jin Z M, Ma H, Li D, Wang L H, Ma G H, Guo F and Chen J 2011 *Appl. Phys. B* **104** 59
[22] Aramburu J A, Moreno M, Doclo K, Daul C and Barriuso M T 1999 *J. Chem. Phys.* **110** 1497
[23] Harris D, Loew G H and Komornicki A 1997 *J. Phys. Chem. A* **101** 3959
[24] Sherman D M 1985 *Phys. Chem. Miner.* **12** 161
[25] Thomsen C, Grahn H T, Maris H J and Tauc J 1986 *Phys. Rev. B* **34** 4129
[26] Ruello P, Pezeril T, Avanesyan S, Vaudel G, Gusev V, Infante I C and Dkhil B 2012 *Appl. Phys. Lett.* **100** 212906
[27] Chen P, Lee N, McGill S, Cheong S W and Musfeldt J L 2012 *Phys. Rev. B* **85** 174413
[28] Morin F J 1951 *Phys. Rev.* **83** 1005